Biogeosciences Discuss.,
https://doi.org/10.5194/bg-2019-149-AC1, 2019

Biogeosciences Discussions
Open Access
EGU

Interactive comment on "Variable C/P composition of organic production and its effect onocean carbon storage in glacial model simulations" *by* Malin Ödalen et al.

Malin Ödalen et al.

malin.odalen@misu.su.se

Received and published: 14 October 2019

1 Introduction

We thank Anonymous Referee #1 for the helpful comments and for the compliments on our paper. In this response, we will respond to the comments by the referee in the order the commented parts appear in the manuscript.

Printer-friendly version

Discussion paper

2 General comments

- ***Introduction: It might be good to add a sentence detailing the evidence for lower terrestrial carbon storage during glacial times (p2, L.1).***
  We agree and will add to the introduction: *Studies of paleoproxy records indicate that carbon storage in the glacial terrestrial biosphere was smaller compared to in interglacial climate* (Shackleton, 1977; Duplessy et al., 1988; Curry et al., 1988; Crowley, 1995; Adams and Faure, 1998; Ciais et al., 2012; Peterson et al., 2014).

- ***Section 2.3.1: It would be good to precise whether the wind changes impact the air–sea gas exchange of CO_2.***
  Yes. In cGENIE, gas transfer velocities are calculated as a function of wind speed (described in Ridgwell et al., 2007), and following Wanninkhof (1992). We will add this information to Section 2.3.1.

- ***Methods and section 3.2.1: If I understand correctly global salinity is not increased during glacial times. If correct, it might be good to clearly state it as well as its impact on solubility changes.***
  This is correct. We do not aspire to simulate a full glacial state, but rather to explore the effect of flexible C/P for biological carbon capture in response to a few common glacial forcings. As we do not change salinity, we are likely to overestimate the increase in solubility between $Ctrl$ and GL_{comb}, by ~ 6 ppm (Kohfeld and Ridgwell, 2009). This effect is consistent for any choice of C/P parametrisation, and is therefore not explored further. We will add this information to Section 3.2.1.

- ***Section 3.2.3: p. 10, L. 29: Please quantify magnitude and direction of "small".***
  We will clarify the sentence by changing it to: *Increases in RLS cause very small, but global, decreases in surface PO_4 concentrations (global average anomaly =*

-0.016 μM) [...]

- ***Section 3.2.3: p. 11, L. 3–4: This is an interesting result that should be emphasized.***
  We add here: *The potential implications of this result for warm climate scenarios is further discussed in Section 4.1.*
  In Section 4.1, we add: *Our sensitivity experiments $RLS \times 0.75$ and $RLS \times 1.25$, reveal that the response in pCO_2^{atm} to the perturbation is enhanced in GAM compared to RED for both increased and decreased RLS. While increased RLS would be an effect of ocean cooling, and thus of interest for glacial studies, reduced RLS would be a consequence of ocean warming (Matsumoto, 2007). Matsumoto (2007) describes how decreased RLS would have a positive feedback on pCO_2^{atm} in future warming climate. Our results imply that flexible C/P could have a further re–inforcing effect on this feedback. It would therefore be of interest to apply a parametrisation of flexible C/P in models used for simulations of future climate feedbacks.* We also add the following sentence to Conclusions: *Flexible C/P also has the potential to be an additional positive feedback of ocean warming on pCO_2^{atm} in future climate.*

- ***Section 3.2.3: p. 10, L. 31–32: This sentence is unclear.***
  We suggest clarifying this sentence by changing it to: *Experiments with deeper RLS in 121 ($RLS \times 1.25_{121}$ and $RLS \times 1.75_{121}$), suggest that about 40 % of the observed differences in pCO_2^{atm} between GAM and RED can again be attributed to the difference in export flux average C/P.*

- ***Section 3.2.3: p. 11, L. 11: Shouldn't iron fertilization lead to an increase in Prem (instead of P^*)?***
  As $\overline{P^*} = \overline{P_{rem}}/\overline{P_{tot}}$, and P_{tot} is constant, an increase in P_{rem} is equal to an increase in P^*. We will clarify the sentence by changing it to: *[...] the iron added by the dust forcing allows more efficient usage of P in the HNLC-regions, which*

increases the ocean storage of biologically sourced carbon P_{rem} (thus, P^* increases).

- ***Section 3.2.3: p. 11, L. 16: It is unclear what you mean here with "radionuclide proxy data"***
  We will clarify the sentence by changing it to: *This subantarctic increase in biological efficiency is consistent with radionuclide proxy data (^{10}Be, ^{230}Th, ^{231}Pa) from the LGM [...].*

- ***Section 4.2: - Please consider amending the title of that section - I would suggest to add all the results of experiment 121 here and thus all the finishing sentences of the diverse paragraph (ex: p. 10, L. 31–32).***
  We agree that grouping all the results of experiment 121 and the associated discussion in Section 4.2 is a good idea, and will follow this recommendation. We will thereby also change the title of the subsection to *Effect of modified but fixed C/P*.

- ***Figure 5: I'm confused as to what is shown here. I think mistakes have been made in the plots or legends as it does not make any sense. How can both HOL and LGM can be shown for CTR? How can both HOL and LGM can be shown for GLcomb? It is really not obvious LGM Pacific is HOL Pac -0.32‰ (h compared to f). Similarly, how do you go from Hol Pac to LGM Pac in CTR (g compared to e)? g looks much more like an Atlantic section than a Pacific one. How can d be LGM Atl and f) Hol Pac? d) might be Pacific.***
  In this figure, the sub–panels have by mistake been shifted to the wrong positions, which naturally causes unnecessary confusion. We apologise for the mistake and show in Fig. 1 the corrected version of the figure, which will replace Fig. 5 in the revised manuscript. The referee is also confused by how both time slices HOL and LGM can be shown for the $Ctrl$-simulation. This is simply because we have chosen to compare each of the simulations ($Ctrl$ and $GLcomb$) with

both time slices (HOL and LGM) of the proxy data. Even though we expect, of course, that $Ctrl$ should to a higher extent reproduce the patterns we see in the HOL data than in the LGM data, we do not want to assume that the model is successful in this respect. For transparency in the process, we therefore show both comparisons. In order to present this figure in a more accessible way, we will clarify that the columns represent the two model simulations, and that the rows represent the proxy records to which we compare the simulations (see updated caption on page C9 of this comment). Note that the update of the caption will also apply to Fig. S3.

Also, it seems the referee may have misunderstood our subtraction of -0.32‰, though the confusion may be a result of the panels being organised in the wrong order. The contours in panel f shows the Pacific Ocean of the $GLcomb$ simulation compared to HOL Pacific proxy records (circles). The contours in panel h also shows the Pacific Ocean of the $GLcomb$ simulation, but here, 0.32‰ has been subtracted from the simulation data. In panel h, the circles show LGM Pacific proxy records. We describe in Section 2.4 that proxy records of $\delta^{13}C$ indicate that the LGM ocean was more depleted in $\delta^{13}C$ than the Holocene ocean. We will clarify that this is also true for the dataset we use here (see Peterson et al., 2014). Gebbie et al. (2015) estimated this difference in whole–ocean $\delta^{13}C$ to -0.32$\pm$0.20‰. The low LGM whole–ocean value is attributed to glacial contraction of the terrestrial biosphere, and an associated addition of $\delta^{13}C$–depleted carbon of terrestrial origin to the ocean. As we do not simulate this terrestrial contribution of $\delta^{13}C$–depleted carbon, we do not expect our $GLcomb$–simulations to reproduce this change in whole–ocean $\delta^{13}C$. We therefore subtract 0.32‰ from each point of the $GLcomb$ simulation output, before we compare to the LGM proxy records.

- ***Figure 9: With a fixed Redfield ratio AC_{rem} should increase with P_{rem}. I am confused as to why AC_{rem} increases with P* here.***

As stated above, $\overline{P^*} = \overline{P_{rem}}/\overline{P_{tot}}$, thus an increase in P_{rem} is analogous to an increase in P^*.

- ***Table 2: I find the format of this table not ideal and wonder if it would make sense to split the RED and GAM results. Also, it might not be necessary to show the AMOC strength for both experiments. The AABW transport in the Atlantic is extremely low (where did you take it?).***
  We agree, and will re–organise the table to show the GAM results below RED results, rather than showing them side by side. However, if the results are presented on different rows, the table would look incomplete if we out the AMOC strength for one of the model versions. We would therefore prefer to keep those results in the table. ψ_{min} in this table is simply the minimum of the Atlantic overturning streamfunction below below 556m depth and north of 30°N. As seen in Fig. 2 c–d, the AABW circulation is weak in the Atlantic north of 30°N, while its peak strength is located in the Southern and Pacific Oceans. Due to the lack of a boundary between the Atlantic and the Pacific south of 30°N, it is not possible to compute the basin–specific streamfunction further south, though the Atlantic AABW circulation is likely to be stronger there.

3 Minor points and typos

- ***Section 2.3.3, p. 6, L. 17: Missing table number***
  Here, *Table ??* should be corrected to *Table 2*.
- ***Section 2.3.3, p. 6, L. 22:***
  Typo, *retreived* should be corrected to *retrieved*.
- ***Section 2.5, p. 7, L. 13:***
  Missing reference marked by *(?)* should be (Ödalen et al., 2018).

- ***Section 3.1.1, p. 8: Sverdrup is usually noted "Sv".***
  SV will be changed to *Sv* throughout the paper.
- ***Section 3.2.4, p. 11, L. 10: remove one "the".***
  Typo, will be corrected.

Printer-friendly version

Discussion paper

4 References

Bouttes, N., Paillard, D., and Roche, D.: Impact of brine-induced stratification on the glacial carbon cycle, Climate of the Past, 6, 575–589, 2010.

Bouttes, N., Paillard, D., Roche, D. M., Brovkin, V., and Bopp, L.: Last Glacial Maximum CO_2 and $\delta^{13}C$ successfully reconciled, Geophysical Research Letters, 38, 2011.

Bouttes, N., Roche, D. M., and Paillard, D.: Systematic study of the impact of fresh water fluxes on the glacial carbon cycle, Climate of the Past, 8, 589–607, https://doi.org/10.5194/cp-8-589-2012, https://www.clim-past.net/8/589/2012/, 2012.

Matsumoto, K.: Biology-mediated temperature control on atmospheric pCO2 and ocean biogeochemistry, Geophysical Research Letters, 34, 2007.

Ödalen, M., Nycander, J., Oliver, K. I. C., Brodeau, L., and Ridgwell, A.: The influence of the ocean circulation state on ocean carbonstorage and CO_2 drawdown potential in an Earth system model, Biogeosciences, 15, 1367–1393, https://doi.org/10.5194/bg-15-1367- 2018, https://www.biogeosciences.net/15/1367/2018/, 2018.

Peterson, C. D., Lisiecki, L. E., and Stern, J. V.: Deglacial whole–ocean $\delta^{13}C$ change estimated from 480 benthic foraminiferal records, Paleoceanography, 29, 549–563, 2014.

Ridgwell, A., Hargreaves, J. C., Edwards, N. R., Annan, J. D., Lenton, T. M., Marsh, R., Yool, A., and Watson, A.: Marine geochemical data assimilation in an efficient Earth System Model of global biogeochemical cycling, Biogeosciences, 4, 87–104, 2007.

Ridgwell, A. J.: Glacial–interglacial perturbations in the global carbon cycle., Ph.D. thesis, University of East Anglia, 2001.

Zeebe, R. E. and Wolf-Gladrow, D. A.: CO_2 in seawater: equilibrium, kinetics, isotopes, 65, Gulf Professional Publishing, 2001.

5 Figures

5.1 Fig. 5 - updated caption

Model ocean $\delta^{13}C$ (contours) compared to the two proxy record time slices (HOL and LGM) of benthic $\delta^{13}C$ (circles) of Peterson et al. (2014). The upper half of the figure shows the Atlantic Ocean (panels a–d), while the lower half shows the Pacific Ocean (panels e–h). The columns represent the model simulations ($Ctrl_{RED}$ or $Ctrl_{GAM}$), while each row represents one of the proxy record time slices (HOL or LGM). The left hand column shows $Ctrl_{RED}$ (panels a, c, e, g), and the right hand column shows $GLcomb_{RED}$ (panels b, d, f, h). The rows show, from top to bottom, a–b) HOL Atlantic, c–d) LGM Atlantic, e–f) HOL Pacific, g–h) LGM Pacific. Note that, before we compare $GLcomb_{RED}$ to LGM observations (panels d and h), a constant of 0.32 ‰ is subtracted from the simulated $\delta^{13}C$, to account for terrestrial release of $\delta^{13}C$–depleted terrestrial carbon which is not modelled. The corresponding comparison for model version GAM is shown in Fig. S.3.

Interactive comment on Biogeosciences Discuss., https://doi.org/10.5194/bg-2019-149, 2019.

Printer-friendly version

Discussion paper

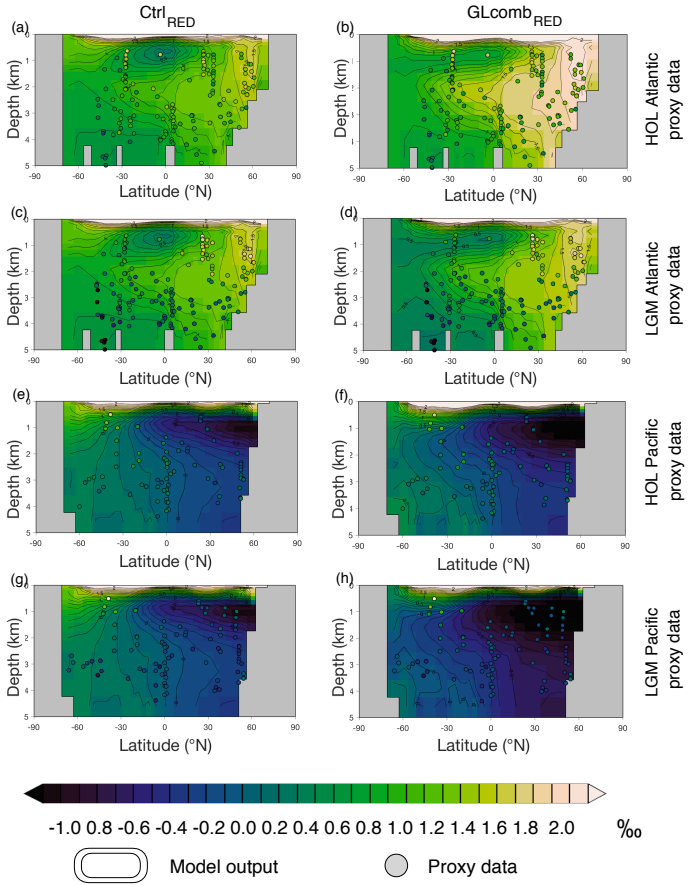

Fig. 1. Updated version of Fig. 5. The caption of Fig. 5 is updated according to the text on the previous page. on

Printer-friendly version

Discussion paper